

Identified two-hadron correlations at STAR using Λ , $\bar{\Lambda}$, and K_{Short}^0 triggers with charged hadrons in Au + Au collisions at $\sqrt{s_{NN}} = 200$ GeV

L. Gaillard^a for the STAR Collaboration

School of Physics and Astronomy, University of Birmingham, Edgbaston, Birmingham, B15 2TT, UK

Received: 6 August 2006 /

Published online: 28 November 2006 – © Springer-Verlag / Società Italiana di Fisica 2006

Abstract. Here we present initial studies of two-dimensional angular correlations of Λ , $\bar{\Lambda}$, and K_{Short}^0 triggers with unidentified charged hadrons in Au+Au collisions at $\sqrt{s_{NN}} = 200$ GeV measured by STAR. Distributions of pseudo-rapidity difference, $\Delta\eta$, and azimuthal separation, $\Delta\phi$, are constructed containing structures observed in unidentified hadron correlations, including a jet peak at small $\Delta\eta$ - $\Delta\phi$ accompanied by a flow-like ridge extended over $\Delta\eta$. These features are studied as a function of centrality via integrated yields and fitting to projections onto $\Delta\eta$ and $\Delta\phi$ axes. Yields are found to be consistent with unidentified correlation analyses, and no clear distinction is observed between the three species.

PACS. 25.75.Gz

1 Introduction

Since 1999 the relativistic heavy ion collider [1] has operated as the world's first collider facility dedicated to the study of nuclear matter under extreme temperatures and energy densities. A large Au+Au data set at $\sqrt{s_{NN}} = 200$ GeV taken in 2004 has made it possible to study the detailed behaviour of the system, and the characteristics of the early fireball are now gradually being revealed [2]. Two-particle azimuthal correlations have provided a highly successful analysis technique which is sensitive to jet-like processes originating in the initial nuclear collisions. Early studies identified the significant suppression of pairs near $\Delta\phi = \pi$ in central heavy-ion collisions with the attenuation of high-momenta particles traversing the medium [3, 4], and now high statistics investigations are uncovering new evidence for the interaction of energetic particles with the bulk. These analyses also benefit greatly from a large acceptance detector, and with a full azimuthal coverage and pseudorapidity acceptance of $|\eta| < 1.8$ for charged particles, the time projection chamber (TPC) at the Solenoidal Tracker At RHIC (STAR) [5] is ideally suited to analyses of this nature.

In this paper we introduce $\Delta\eta - \Delta\phi$ correlations, and present the early results of an analysis involving identified trigger correlations. The features observed in $d + \text{Au}$ collisions are defined and then used to identify the additional structures found uniquely in central heavy-ion collisions.

Identified correlations are proposed as a means to understand the mechanisms responsible for these structures. In Sects. 3 and 4, two developing analyses of correlations are described involving identified Λ , $\bar{\Lambda}$, and K_{Short}^0 triggers with unidentified associated charged tracks.

2 Jet tomography

Full jet reconstruction on an event by event basis is not possible in the high-multiplicity environment of a relativistic heavy-ion collision, as jet products are indistinguishable from the underlying event. Two-particle angular correlations offer an alternative approach that takes advantage of the kinematics of jet processes as well as the accumulated statistics achieved by summing over a complete data set. The principle relies upon the assumption that the leading particle in a jet carries a significant fraction of the total jet energy and thus lies close to the jet axis (direction of the parton after the initial scatter). Furthermore, other particles in the same event with high transverse momentum, p_T , are likely to be fragments of either the same jet (or di-jet) and therefore will possess some angular relationship with the leading particle. Figure 1 gives a schematic representation of a di-jet overlaying a real Au + Au collision recorded in the STAR TPC.

A typical two-particle correlation routine begins by finding a high- p_T *trigger* particle in an event. The angular distribution of *associated* particles in the event with p_T less than the trigger and above some lower threshold

^a e-mail: lxx866@bham.ac.uk

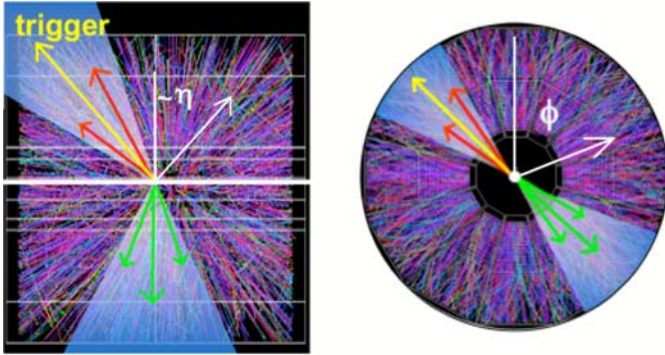


Fig. 1. Schematic representation of a di-jet overlaying a real heavy-ion collision observed in the STAR time projection chamber (TPC). The *left image* shows the projection transverse to the beam axis. The *right image* illustrates the azimuthal projection. *Arrows* represent jet daughter tracks, with lengths indicating momenta

is then formed relative to the trigger, giving a $\Delta\phi$ correlation where $\Delta\phi = \phi_{\text{asso.}} - \phi_{\text{trig.}}$. This is repeated for all trigger particles in that event and then for all events in the data set, and the total correlation is then normalised by the total number of triggers. In STAR, early azimuthal correlation studies involving unidentified charged particles used thresholds of $2.0 < p_{\text{T}}^{\text{asso.}} < 4.0 < p_{\text{T}}^{\text{trig.}} < 6.0$ GeV/c [3]. These were characterised by enhancements near $\Delta\phi = 0$ and $\Delta\phi = \pi$, hereafter labelled same-side and away-side peaks to reflect the relationship between members of the pair. In heavy-ion collisions, the background is modulated by a $\cos(2\Delta\phi)$ elliptic flow contribution.

Two-particle correlations have been extended by including pseudo-rapidity difference, $\Delta\eta = \eta_{\text{asso.}} - \eta_{\text{trig.}}$, providing a second dimension and in effect allowing the jet cone to be mapped out. The limited acceptance in pseudo-rapidity results in a pair-wise acceptance, which appears as an approximately triangular shape in $\Delta\eta$. The pair-wise acceptance approximates to the convolution of the single particle distributions. In Fig. 2a, the raw $\Delta\eta - \Delta\phi$ correlation of unidentified charged particles in $d + \text{Au}$ collisions at $\sqrt{s_{NN}} = 200$ GeV is presented for trigger and associated particles satisfying $2.0 < p_{\text{T}}^{\text{asso.}} < 3.0 < p_{\text{T}}^{\text{trig.}} < 6.0$ GeV/c. In the present analysis, raw correlations – hereafter labelled sibling correlations – were corrected for ac-

ceptance with event mixing. For a given set of triggers, a second correlation was made where associated particles were sourced from other events with primary vertex positions within 10 cm and with similar multiplicities to the event containing the trigger. The resulting correlation reproduces features caused by the detector acceptance, as shown in Fig. 2b. The correction was performed by dividing the sibling correlation by the mixed event on a bin by bin basis, and the result is illustrated in Fig. 2c. Several events were mixed for every trigger particle in order to reduce statistical uncertainties relative to the sibling correlation. This correction also removed a periodic $\Delta\phi$ acceptance feature caused by gaps between the TPC sectors. The same-side peak is localised around $\Delta\eta = 0$, but the away-side peak is extended in $\Delta\eta$. This is in part a consequence of the rest frame of the measurement not coinciding with the rest frame of the hard parton scatter. In addition, back-to-back pairs occupy a range of $\Delta\eta$ depending on the trigger η , and so this further contributes to the smearing of the away-side peak in $\Delta\eta$.

Figure 3 illustrates a correlation involving the same kinematic selection as for the $d + \text{Au}$ correlations above, but for 0–5% central Au + Au at $\sqrt{s_{NN}} = 200$ GeV. The away-side peak is considerably suppressed (elliptic flow has not been subtracted from this figure), and the same-side contains a peak localised around $\Delta\eta = 0$, and a ridge, extending beyond $|\Delta\eta| < 1.5$. The shape of the ridge is similar to the contribution from elliptic flow, however its localisation on the same-side suggests some relationship with the jet process. It has been proposed that the existence of the ridge is evidence for a coupling between the jet and the longitudinally expanding medium [6–8]. The same-side has been studied for unidentified particles [9], where it was found that the ridge yield increases with centrality while the yield of the jet peak appears constant (note normalisation with respect to number of triggers). Moreover, the contribution of the ridge for associated particles with $p_{\text{T}} > 3.0$ GeV/c is small, as would be expected if the underlying mechanism is hydrodynamical in nature.

The same-side ridge occupies an interesting region in transverse momentum where one observes the decline of the hydrodynamical regime [10] and the onset of the baryon - meson difference [11, 12] that has been described in terms of parton recombination. Although trigger particles with $3.0 < p_{\text{T}} < 6.0$ GeV/c should be dominated by thermal recombination, correlations intrinsically provide

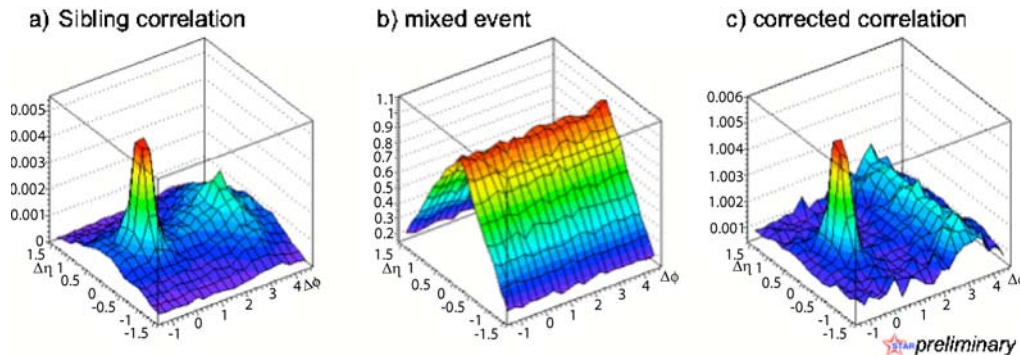


Fig. 2. Unidentified $\Delta\eta - \Delta\phi$ correlations in $d + \text{Au}$ collisions at $\sqrt{s_{NN}} = 200$ GeV. **a** raw (sibling) correlation; **b** mixed event correlation; **c** sibling correlation corrected by mixed event

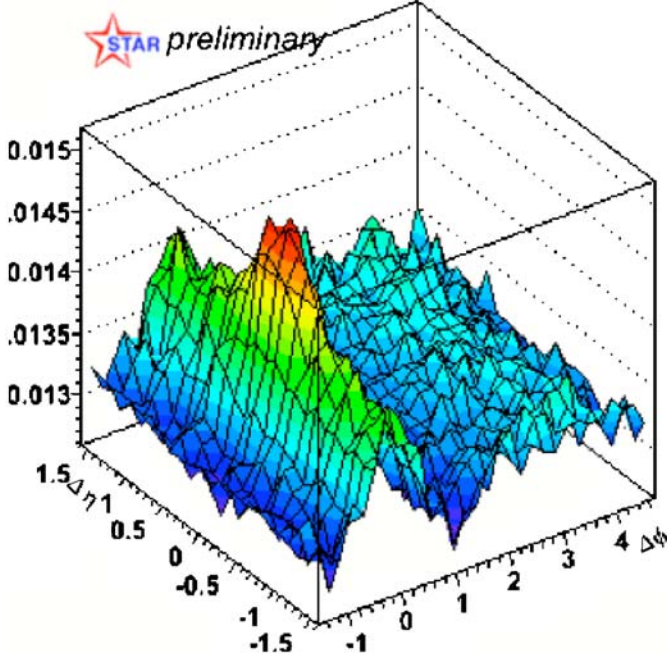


Fig. 3. Acceptance corrected unidentified correlation in 0–5% central Au + Au at $\sqrt{s_{NN}} = 200$ GeV

an increased sensitivity to shower parton contributions. Consequently, identified correlations may yield some indication as to the physics of the same-side ridge, and moreover on the interaction between jet partons and the medium. Mass and species dependencies can be investigated by drawing comparisons between correlations involving different identified trigger and/or associated particles. In this study, Λ , $\bar{\Lambda}$, and K_{Short}^0 (collectively named $V0$ s) are used for this purpose. These are reconstructed via their dominant weak decay channels into pairs of charged particles:

$$\Lambda \rightarrow p^+ \pi^- \quad (BR = 63.9 \pm 0.5)\% \quad (1)$$

$$\bar{\Lambda} \rightarrow p^- \pi^+ \quad (BR = 63.9 \pm 0.5)\% \quad (2)$$

$$K_{\text{Short}}^0 \rightarrow \pi^+ \pi^- \quad (BR = 68.95 \pm 0.14)\% \quad (3)$$

These respectively offer high purity sources of baryons, anti-baryons and mesons in the p_T region of interest. The main disadvantage is one of statistics, given that $V0$ s are considerably rarer than charged particles emanating from the primary vertex. In the present work, correlations of identified triggers are presented, associated with unidentified charged particles.

3 Bin-counting analysis of jet yield

Assuming the ridge yield to be constant as a function of $\Delta\eta$ within the observable range, a ridge independent jet yield was determined by subtracting the same-side yield of pairs at large $\Delta\eta$ from the yield at small $\Delta\eta$, after applying

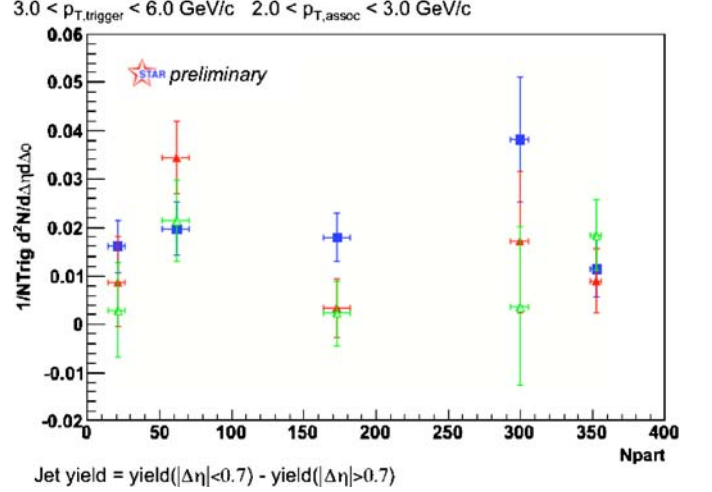


Fig. 4. Jet yields calculated by subtracting $\Delta\eta$ regions on the same side. Marker style represents trigger species: filled triangles for Λ , open triangles for $\bar{\Lambda}$, and square datapoints for K_{Short}^0 triggers

the mixed event correction. The measurement is also independent of (elliptic) flow modulations of the background. Yields were corrected for the reconstruction efficiency of associated particles using a parameterisation from charged track embedding. The correction was applied as a function of p_T and centrality, and integrated over pseudo-rapidity and primary vertex position.

In Fig. 4, meson- and baryon- triggered jet yields are plotted as a function of the number of participants and five centrality classes derived from Glauber model calculations [13]. The data set included approximately 3×10^7 minimum bias Au + Au events defined by zero degree calorimeter (ZDC) coincidences and fast scintillators located within $|\eta| < 1.0$ (central trigger barrel, CTB) [5]. The data-point for 0–5% central in Fig. 4 utilised an online triggered central data set of approximately 3×10^7 Au + Au events with low ZDC counts and high CTB signals corresponding to a centrality selection of 0–10%. Uncertainties remain high in central data relative to more peripheral selections despite better statistics. This is a consequence of the considerably larger contributions to the correlations from non-jet sources.

The jet yield is defined as the number of pairs per trigger within $|\Delta\eta| < 0.7$ less those with $0.7 < |\Delta\eta| < 1.4$. Varying the $|\Delta\eta|$ window from 0.6 to 0.8 did not affect the determined yields within statistical uncertainties. Little centrality dependence was observed for the jet yield. Baryon and meson triggered yields are consistent, although some separation was observed in mid central collisions.

4 Projection analysis

A more direct measurement of the jet yield can be obtained by comparing projections onto $\Delta\eta$ and $\Delta\phi$ axes. Assuming flow and the ridge to be invariant with respect

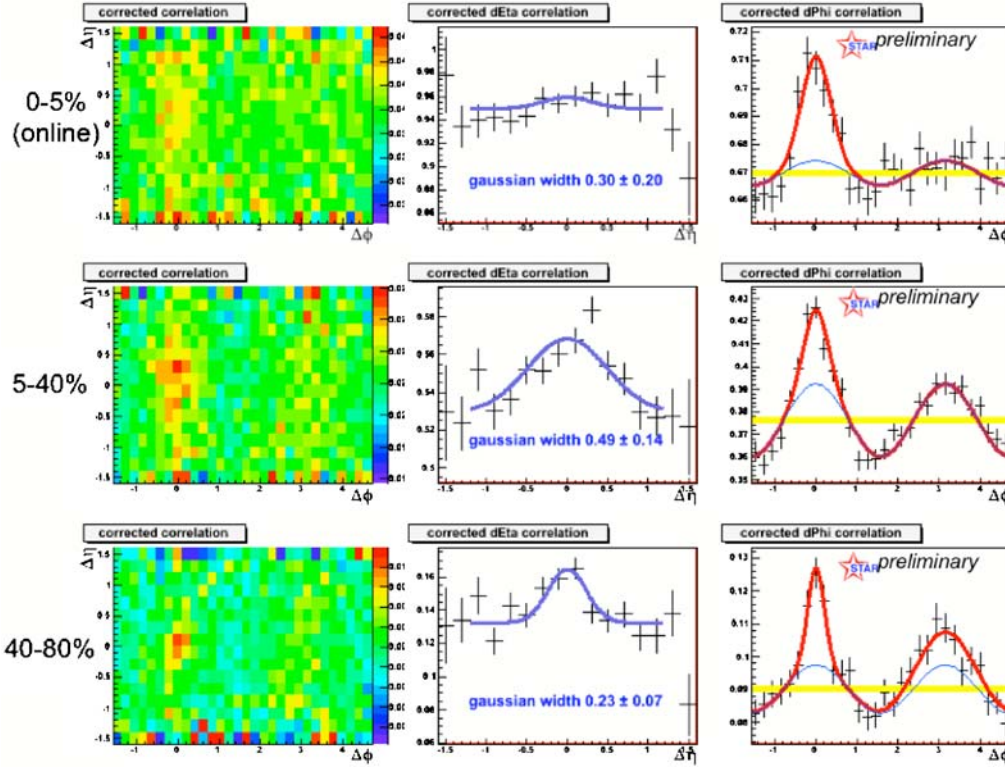


Fig. 5. Projection analysis of $\Delta\eta - \Delta\phi$ correlations with K_{Short}^0 triggers

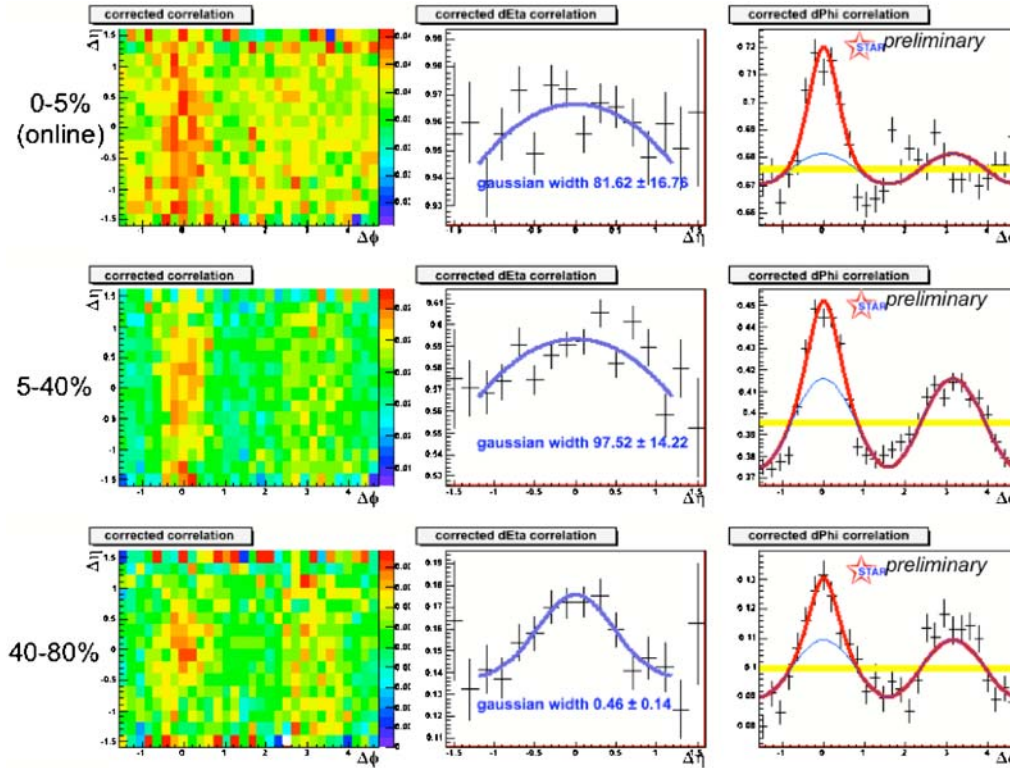


Fig. 6. Projection analysis of $\Delta\eta - \Delta\phi$ correlations with Λ and $\bar{\Lambda}$ triggers

to $\Delta\eta$ (within the range included in this study), a projection of the same-side peak onto $\Delta\eta$ can be described by a Gaussian function located at $\Delta\eta = 0$. Subtracting the yield of this Gaussian function from the same-side yield de-

termined from a $\Delta\phi$ projection provides a measure of the ridge, given a known flow contribution.

Figure 5 shows K_{Short}^0 -triggered $\Delta\eta - \Delta\phi$ correlations and projections. Three centralities are included using the

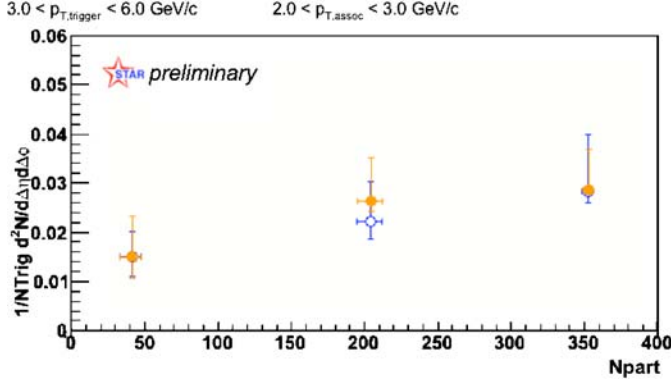


Fig. 7. Same side $\Delta\phi$ yields for meson (open markers) and baryon (filled markers) triggered correlations

minimum bias and online central triggered data set. The projections onto $\Delta\phi$ were fit with the cyclic function

$$\frac{dN}{d(\Delta\phi)} = Ae^{-\frac{1}{2}\left(\frac{\Delta\phi}{\sigma_A}\right)^2} + Be^{-\frac{1}{2}\left(\frac{\Delta\phi-\pi}{\sigma_B}\right)^2} + C(1 + D \cos(2\Delta\phi)), \quad (4)$$

where the Gaussian terms A and B represent the same-side and away-side peaks respectively. The background was modulated by elliptic flow, and the variable D was calculated from a parameterisation of elliptic flow studies, averaging between cumulant and reaction plane results [14]. The level of the valley regions was input as a starting parameter for the background, according to the zero yield at minimum (ZYAM) approach [15].

Statistical uncertainties in the $\Delta\eta$ projections are more significant. A fit was performed consisting of a single Gaussian with mean at $\Delta\eta = 0$, plus a flat pedestal. The fit was poorly constrained in the most central correlation, indicating the peak was too shallow or wide to resolve, thus jet and ridge contributions could not be isolated. Figure 6 shows the equivalent baryon-triggered $\Delta\eta - \Delta\phi$ correlations and projections. The $\Delta\phi$ distributions gave consistent results to the meson-triggered correlations. A comparison of extracted $\Delta\phi$ yields is presented in Fig. 7 which contains contributions from both the ridge and the jet. Yields increase with centrality, reflecting an increasing contribution from the ridge. No species dependence is observed.

Despite similar occupancies, the $\Delta\eta$ correlations with baryon triggers are poorly defined. This may indicate some persistent systematic effect such as the merging of crossing tracks (charge independent unidentified auto-correlations at similar p_T have excluded crossing pairs for this reason [16]). The merging of tracks could account for a suppression in the number of pairs found with small $\Delta\eta - \Delta\phi$, and may be more significant for Λ and $\bar{\Lambda}$ correlations than

for K_{Short}^0 correlations due to the kinematics of the $V0$ decay.

5 Conclusions

Two-particle $\Delta\eta - \Delta\phi$ correlations have been demonstrated in Au + Au collisions at $\sqrt{s_{NN}} = 200$ GeV using Λ , $\bar{\Lambda}$ and K_{Short}^0 triggers reconstructed from $V0$ decay channels. The features found at small $\Delta\phi$ have been studied via comparisons of yields at large and small $\Delta\eta$, and also by $\Delta\eta$ and $\Delta\phi$ projections.

The jet yield appears flat with centrality. The combined jet and ridge yields increase with centrality. These results agree with unidentified correlations, although the extracted jet yields in this study appear systematically lower. Despite some non-statistical differences, no clear species dependence is observed. Systematic effects including track merging are currently under investigation.

This analysis is being extended to include a greater pseudorapidity coverage of $|\Delta\eta| < 2.0$, with the aim of further constraining $\Delta\eta$ projections. Once these studies have been completed for identified trigger correlations, the analysis will advance to the statistically more challenging study of correlations involving identified associated particles.

References

1. H. Hahn et al., Nucl. Instrum. Methods A **499**, 245 (2003)
2. STAR Collaboration, J. Adams et al., Nucl. Phys. A **757**, 102 (2005)
3. STAR Collaboration, C. Adler et al., Phys. Rev. Lett. **90**, 082302 (2003)
4. STAR Collaboration, J. Adams et al., Phys. Rev. Lett. **91**, 072304 (2003)
5. K.H. Ackermann et al., Nucl. Instrum. Methods A **499**, 624 (2003)
6. Armestro et al., Eur. Phys. J. C **38**, 461 (2005)
7. C.B. Chiu, R.C. Hwa, Phys. Rev. C **72**, 034903 (2005)
8. R.C. Hwa, C.B. Yang, Phys. Rev. C **70**, 054902 (2004)
9. STAR Collaboration, J. Putschke, this volume
10. P.F. Kolb, U. Heinz, nucl-th/0305084
11. STAR Collaboration, M.A.C. Lamont, J. Phys. G **30**, S963 (2004)
12. STAR Collaboration, P.G. Jones et al., J. Phys. G **31**, S399 (2005)
13. STAR Collaboration, C. Adler et al., Phys. Rev. Lett. **89**, 202301 (2002)
14. STAR Collaboration, C. Adler et al., Phys. Rev. C **66**, 034904 (2002)
15. N.N. Ajitanand et al., Phys. Rev. C **72**, 011902 (2005)
16. STAR Collaboration, J. Adams, et al., Phys. Rev. C **73**, 064907 (2006)